DOI 10.1007/s11015-016-0178-x
Metallurgist Vol. 59, Nos. 9–10, January, 2016 (Russian Original Nos. 9–10, Sept.–Oct., 2015)

DAMASCUS STEEL MICROSTRUCTURE

D. A. Sukhanov and L. B. Arkhangel'skii UDC 669.141.13

The nature of change in the amount and morphology of iron dendrites and excess phases in relation to the degree of high-carbon alloy melt supercooling is considered. It is revealed that in pure iron-carbon alloys by changing the degree of melt supercooling it is possible to obtain steel with a carbon content as in white cast iron, or white cast iron with a carbon content as in steel. It is shown that before forging Damascus steel the structure is ideal with a pearlite matrix, without secondary free cementite, and with excess ledeburite phase. Features of ferrite and ledeburite shape change with thermomechanical treatment (forging) are studied. It is detected that during deformation heating for forging there is ledeburite recrystallization into a more stable phase of eutectic carbide. Limits are determined for transformation of pure high-carbon alloys in carbide class steel of the Damascus type.
Keywords: *bulat, Damascus steel, wootz, Indian steel.*

Interesting data about the microstructure of ancient bulat objects have been published in Russian language work [1–12]. The authors of these works in essence differ in opinion, although generally they have similar points of view about the bulat steel microstructural components. Other information on this theme has been based on conclusions of this work. It is generally considered that bulat microstructure consists of cold-worked troostite (grain size 0.1 μm) matrix with unevenly distributed coagulated anomalously coarse secondary cementite distributed within it (10–50 μm), or conglomerates of ledeburite distributed within it. In photographs given in this work for the microstructure, it is seen that a considerable part of cementite has a different nature of occurrence. What is the nature of occurrence of this cementite? How does the structure formation process proceed? What are the main differences in bulat microstructure from other high-carbon steels and alloys? The aim of this work is to find answers to these questions.

Structural components of iron-carbon alloys as a rule consist of solid solution (in the form of dendrites) and excess phases, in particular, cementite and ledeburite. A defining factor from the point of view of ductility is structural component purity. All impurities, apart from carbon, should be contained in hundredths or thousandths fractions. Only in this case the amount, morphology, and nature of distribution of iron dendrites and excess phases determines the degree of alloy supercooling.

In the contemporary understanding of alloy cleanliness, the presence within its composition of residues of products of manganese or silicon deoxidization is not excluded. With the presence of manganese, more than 0.2% austenite dendrite growth is delayed during alloy solidification, there is a change in carbide composition, and pearlite is stabilized during high-temperature annealing. Silicon, even with a content of only 0.2%, creates graphitizing centers. With alloy supercooling, metastable cementite is formed capable of breaking down on heating for forging with the formation of graphite and austenite.

In order to exclude the unfavorable effect of the deoxidation factor, in the research and production base of the Bardin TsNIIchermet on the initiative of L. B. Arkhangel'skii, experiments have been carried out for melting in a crucible high-carbon alloys in a vacuum furnace without deoxidation. The chemical composition of high-carbon alloys of types BU16A, BU22A, and BU27A is given in Table 1. In alloy grading, letters and numbers signify the following: BU is carbon bulat containing not more than 0.1% manganese and silicon (each individually); 16 is the average carbon weight fraction (1.6 wt.%); A is a high-quality alloy containing not more than 0.03% sulfur and phosphorus (each individually); all of the rest of the elements in

ASK-MSTs Company, Moscow, Russia; e-mail: suhanov7@mail.ru, tigram.korolev@mail.ru. Translated from Metallurg, No. 9, pp. 72–75, September, 2015. Original article submitted May 6, 2015.

TABLE 1. Test High-Carbon Alloy Chemical Composition

Alloy	Content, wt.%				
	C	Si	Mn	P	S
BU16A	1.62	0.069	0.026	0.002	0.004
	rest of elements in hundredth or thousandth fractions				
BU22A	2.25	0.065	0.024	0.002	0.004
	rest of elements in hundredth or thousandth fractions				
BU27A	2.70	<0.10	<0.10	0.003	0.003
	rest of elements in hundredth or thousandth fractions				

TABLE 2. Structure of Alloys BU16A, BU22A, BU27A

Alloy grading	Production process	Alloy microstructure
BU16A	Vacuum melting, alloy air cooling (+20ºC)	Pearlite + cementite II in form of needles (10%)
BU22A		Pearlite + cementite II in form of needles (20%)
BU27A		Pearlite + cementite II in form of needles (10%) + ledeburite (20%) in form of network
BU16A	Crucible melting, soaking 5 h at 1200ºC, furnace cooling	Pearlite + ledeburite (10%)
BU22A		Pearlite + ledeburite (20%)
BU27A		Pearlite + ledeburite (30%)

hundredths or thousandths fractions. The carbon content in these alloys was selected from the following considerations. We were interested in the behavior of structural components of high-carbon alloys in the field of transfer of an alloy from a composition corresponding to steel into a cast iron type composition. By changing in this range the degree of alloy melt supercooling, it is possible to obtain steel with a carbon content both in white cast iron or white cast iron containing carbon, as in steel.

During alloy melting in a vacuum, the degree of melt supercooling is quite high, since a crucible is cooled at room temperature (+20C). The structure of BU16A and BU22A alloys (Table 2) is finely dispersed matrix of lamellar pearlite with excess needles of Widmanstätten cementite arranged within it of about 10 and 20 vol.%, respectively. In alloy BU16A, the needled thickness of Widmanstätten cementite is about 3–5 μm, and in alloy BU22A about 7–10 μm. The predominant precipitation of cementite of the Widmanstätten type is explained by the fact that with an increase in degree of alloy supercooling there is a reduction in the critical size of nuclei and an increase in amount of crystallization centers. In alloy BU27A, apart from cementite of the Widmanstätten type, a network of ledeburite distributed between dendrites is observed (volume fraction about 20%). The thickness of excess ledeburite phase varies within limits of 20–30 μm. For all alloys without exception, the magnitude of dendrites is about 50–100 μm.

Alloys with this structure are poorly amenable to plastic deformation. The metal is not ductile, subject to crack formation, and is dampened during forging. This is due to the fact that excess cementite formed as a result of austenite recrystallization has a layered structure. During deformation, cementite splits down over layers, creating additional stress concentration centers. The round particles of cementite obtained retain orientation in the immediate vicinity of original layered platelets, forming fine patterns. The set of properties with these quasibulat steels is low, although hardness after stepwise hardening and low-temperature tempering may reach 63–64 HRC.

As noted in [13], in order to improve the set of production properties, it is necessary to convert excess Widmanstätten cementite into another structural component. The ideal structure before forging is a pearlitic matrix with excess ledeburite

a *b* *c*

Fig. 1. Alloy BU27A ledeburite morphology (×1100): *a*) lamellar, unmodified; *b*) lamellar, modified (<0.1% Al); *c*) modified (0.02% Ca).

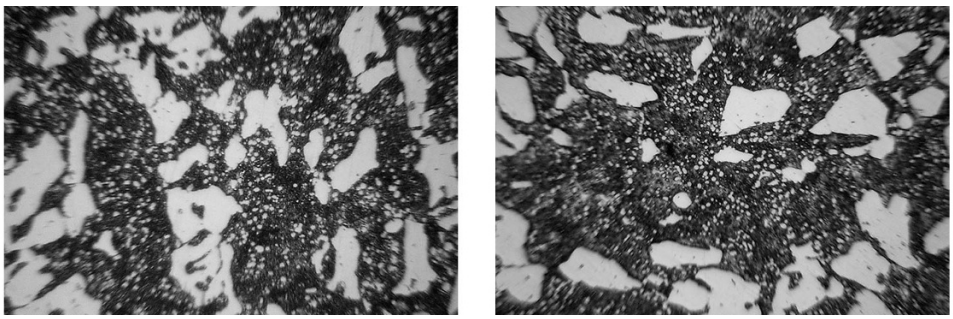

a *b*

Fig. 2. Alloy BU27A eutectic carbide morphology (×900) after specimen forging: *a*) with ledeburite lamellar structure (sorbite matrix (0.2 μm) + quasiledeburite (20–50 μm) + eutectic cementite (10–20 μm)); *b*) specimen with ledeburite cellular structure (sorbite matrix (0.2 μm) + eutectic cementite (10–30 μm)).

phase (without free secondary cementite). This problem may be resolved by melt slow cooling, for example, crucible melting with exposure for 5 h at 1200ºC, followed by furnace cooling (see Table 2). With slow cooling of high-purity iron-carbon alloy, there is formation of a coarser structure of austenite dendrites impoverished in carbon (not more than 0.8% C). The interdendritic parts are enriched with carbon up to eutectic content, even in alloys not found according to the composition diagram in the cast iron zone. This effect was noted in work of Gaev [2].

Three main morphological types of ledeburite eutectics exist: lamellar (Fig. 1*a*), lamellar-cellular (Fig. 1*b*), and cellular (Fig. 1*c*). The most widespread ledeburite eutectic is lamellar-cellular, since with an increase in the degree of alloy supercooling the volume fraction of ledeburite with a lamellar structure increases sharply.

This situation may be changed by adding a modifying addition to the alloy. For example, introduction into the alloy of up to 0.10% aluminum facilitates predominant formation of lamellar ledeburite. Introduction into alloy of up to 0.02% calcium (as a modifier) facilitates the formation of ledeburite of a predominantly cellular type. Ledeburite of this morphology exhibits the greatest ductility in the intercritical range of melting. Additionally there is austenite grain refinement, formation of secondary cementite Widmanstätten structure is suppressed, and this facilitates the formation during forging of carbide inclusions of prismatic and circular shape with a size of 10–30 μm.

We consider how alloy deformation with excess ledeburite proceeds. At first, austenite deforms, and dislocations accumulate around ledeburite. Ledeburite is under the action of normal compressive stresses and shear strain stresses caused by forces of adhesion at the ledeburite-austenite interface. Significant dislocation density within ledeburite leads to dynamic recrystallization with the formation of eutectic carbides.

During deformation of lamellar and lamellar-cellular ledeburite, energy is consumed in splitting platelets over contact zones, and then repeated consumption in secondary recrystallization in eutectic carbide that is difficult to deform. The process

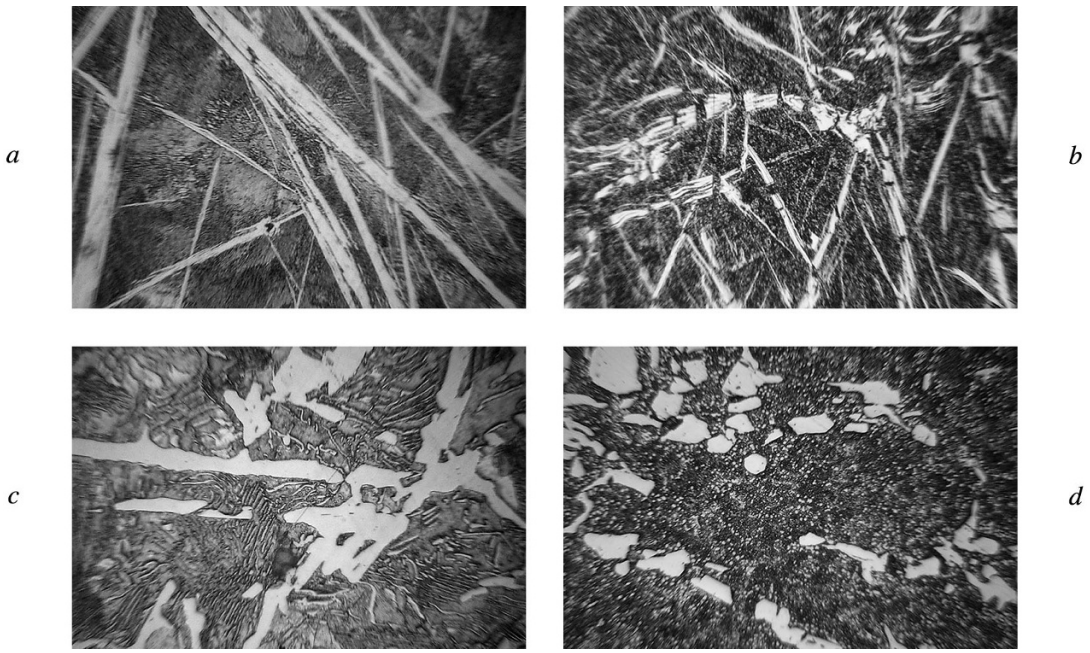

Fig. 3. Alloy BU22A morphology: with Widmanstätten structure (×1000) before (*a*) and after forging (*b*) (×800); with excess ledeburite phase (×1000) before (*c*) and after forging (*b*) (×1000).

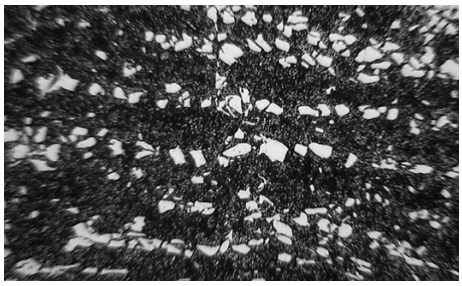

Fig. 4. Alloy BU22A nature of eutectic carbide distribution and morphology (×300).

is incomplete in nature. The majority of carbides have a near-rectangular shape (Fig. 2*a*). During deformation of cellular ledeburite, energy is at first consumed in recrystallization in eutectic carbide that is difficult to deform (Fig. 2*b*). It may be suggested that an alloy containing ledeburite in cellular form should exhibit the greatest ductility in a hot condition. This assumption is confirmed by torsion tests carried out in [14] on test specimens of alloyed material with eutectics of different morphological types. This may confirm the fact that on heating for forging there is ledeburite recrystallization into a more stable phase of eutectic carbide. A ductility peak is observed in this intercritical temperature range.

For comparison, we consider the microstructure of alloy BU22A. The alloy structure is shown in Fig. 3 with a Widmanstätten component before and after forging. It is seen how cementite needles are split over areas of layers in contact, and separate during deformation into individual fragments. The alloy's structure is similar to growths of an impenetrable bush, which points to the low structural strength and cutting capacity. The alloy structure is shown in Fig. 3*c*, *d* with a quasiledeburite structure of cementite before and after forging. All of the deformation energy accumulated in the process at an austenite–quasiledeburite interface initiates quasiledeburite structure recrystallization with formation of new (eutectic) cementite. This cementite does not have a layered structure, and its particles have a prismatic shape and high decomposition

temperature of more than 1150ºC. Grains of eutectic type at the head of a wedge will be arranged in the forging direction, as shown in Fig. 4. The completed process of ledeburite recrystallization is irreversible and it is comparable with artificial alloy ageing. The properties of alloy BU22A with a work-hardened troostite matrix and excess eutectic cementite phases may compete with the properties of forged steels of type X12. The difference only consists in the chemical composition of excess cementite phases.

Conclusion. The limits of high-carbon alloy steel transformation into steel of a carbide type of bulat have been determined. The lower limit should be alloy composition with a degree of eutectic not less than 5%, which corresponds to a carbon content of not less than 1.2%. Due to the fact that ledeburite is arranged at internodes in the form of bunches not connected with each other, at the surface of a bulat steel specimen after forging a banded pattern appears which corresponds to bulat of the lowest type of "sham." For the upper boundary of formation of hypereutectic alloys in bulat criteria may be used with which contact between solid solution dendrites is still possible. This contact appears in alloys with a degree of eutectic lower than 30%, which corresponds to a carbon content of 2.5–2.7% [15]. After forging this alloy at the surface coarse articulated patterns of complex configuration of the Taban or Horosan types predominate [16].

REFERENCES

1. P. P. Anosov, "Bulats," in: *Russian Scientists – Metallurgists*, D. M. Nakhimov and A. G. Rakhstadt (eds.), GNTI Mash.. Lit., Moscow (1951), pp. 38–112.
2. I. S. Gaev, "Bulat and contemporary iron-carbon alloys," *MiTOM*, No. 9, 17–24 (1965).
3. F. N. Tavadze, V. G. Amaglobeli, and G. V. Inashvili, "Study of bulat steel," *Soobsh. AN GSSR*, **115**, No. 3, 589–592 (1984).
4. O. D. Sherby and J. Wadsworth, "Damascus steel," *V Mire Nauki*, No. 4, 74–80 (1985).
5. V. I. Basov, "Bulat: lifeline," *Metallurg*, No. 7, 16–23 (1991).
6. A. M. Parshin and N. B. Kirillov, "Role of Fe_3C carbide distribution uniformity in bulat steel," in: *Radiation Damage and Alloy Properties*, A. M. Parshin and A. N. Tikhonov (eds.), Politekhnika, Moscow (1995), pp. 32–40.
7. Yu. G. Gurevich, "Classification of bulat with respect to macro- and microstructure," *MiTOM*, No. 2 (620), 3–7 (2007).
8. V. M. Schastlivtsev, V. Yu. Gerasimov, and D. P. Rodionov, "Structure of three golden bulats," *FMM*, **106**, No. 2, 182–188 (2008).
9. V. V. Kuznetsov, "Bulats," *Kalashn. Oruzhie, Boepr., Snaryazh.*, No. 1, 82–85 (2007).
10. I. Taganov, "Setting of bulat legend," *Kalashn. Oruzhie, Boepr., Snaryazh.*, No. 11, 92–97 (2009).
11. L. B. Arkhangel'skii, "Bulat grades," *Klinok*, No. 21, 18–27 (2011).
12. V. M. Schastlivtsev, V. M. Urtsev, A. V. Shmakov, et al., "Structure of bulat," *FMM*, **114**, No. 7, 650–657 (2013).
13. D. A. Sukhanov, "Bulat – carbide class unalloyed steel," *Metallurg*, No. 2, 93–96 (2014).
14. Yu. N. Taran, P. F. Nizhnekovskaya, T. M. Mironova, et al., "Structural changes in eutectic steels R6M5 with hot plastic deformation," *Izv. Vyssh. Uchebn. Zaved., Cher. Met.*, No. 5, 109–113 (1981).
15. P. F. Nizhnikovskaya, "Structure and ductility of eutectic type iron-carbon alloys ," *MiTOM*, No. 9, 5–9 (1984).
16. A. V. Arkhangel'skii, *Secrets of Bulat*, Metallurgiya, Moscow (2007).